ZIBELINE INTERNATIONAL™ PUBLISHING

ISSN: 2773-6202 (Online)
CODEN: JTIOCC

Journal of Technology & Innovation (JTIN)

DOI: http://doi.org/10.26480/jtin.02.2023.61.71

RESEARCH ARTICLE

CONSIDERATION OF DAMAGING FREQUENCY RANGES OF STRUCTURAL EXCITATION FOR TESTING LARGE BATTERY PACKS IN BATTERY ELECTRIC VEHICLES (BEV)

Benedikt Plaumann

Hamburg University of Applied Sciences (HAW Hamburg), Faculty of Engineering and Computer Science, Department of Automotive and Aeronautical Engineering, 20099 Hamburg, Germany.
Corresponding Author Email: benedikt.plaumann@haw-hamburg.de

ARTICLE DETAILS

Article History:

Received 25 May 2023
Revised 28 June 2023
Accepted 01 August 2023
Available online 08 August 2023

ABSTRACT

Realistic vibration testing of large floor mounted Battery Pack, sometimes called Rechargeable Energy Storage Systems (RESS), for Batterie Electric Vehicles (BEV) is important for developing safe new battery structures. On the other hand, the requirements for realistic replications of worst-case environments in a lab usually demand costly and complex infrastructure. A key factor to the quality of environment replication and an important cost driver due to the increasing complexity is the needed frequency range the equipment must be able to replicate. The contribution analyzes data from a first pre-test campaign to demonstrate a feasible process of deriving frequency band requirements for the test equipment. The key method used here is the Fatigue Damage Spectrum (FDS) to analyze the potential damage a vibration could cause in certain failure mechanism of interest, particularly "weighted" by the corresponding double-logarithmic dependance of stress magnitude over occurring load cycles. This enables a good assessment of how much damage could be induced in certain frequency ranges for a well justified and cost-effective choice on the needed test equipment.

KEYWORDS

Battery Electric Vehicle, BEV, Vibration Spectrum, Fatigue Damage Spectrum, Battery Pack, Rechargeable energy storage system, RESS

1. INTRODUCTION

Vibration Testing is an important task for ensuring high reliability, especially in environments that may cause critical damage to a technical system. As for Battery Electric Vehicles (BEV), Battery Pack or the Rechargeable Energy Storage System (RESS) is typically composed of several hundred to thousands of Lithium-Ion Battery Cells. These may pose a potential fire risk when mechanical environments cause an internal or external electrical short-circuit occurs, which may be induced by a mechanical deformation or mechanical contact of power conducting subcomponents of a battery, the cables or the corresponding power electronics. (Sun et al., 2020)

Hence, the safety critical battery components are typically tested on various levels from cell, over module to battery pack / traction battery, mainly depending on the design scope at a given step in the design process. Tests on vehicle level are then finally undertaken for high-level verification and validation. While this can only be done with a carrier vehicle very similar to the later production car (only available at a very late stage), a lab test allows to adapt the induced mechanical environment to assumed changes in vibration excitation regarding battery-vehicle-interaction, vehicle design and road surfaces. The battery packs as the largest single component of the power train and one of the most critical in safety assessment poses special requirements towards component testing in a lab (Plaumann, 2022). For defining a suitable test procedure, many technical parameters like maximum deflection, maximum velocity, maximum acceleration, mechanical interface impedances and guidance stiffness depend on the frequency range of the vibration excitation deemed most relevant. Component tests on such high levels (large composed structures) typically target mainly the verification of mechanical durability and fatigue under excitation similar to assumed worst-case real-world environments. Therefore, the fatigue damage is seen as the most relevant influence for defining a relevant frequency range of the test in the lab.

2. STATE OF THE ART

High performance and a sufficient safety of a product design always depend on valid load assumptions, matching requirements and thorough verification and validation. As current BEV do not show a higher risk of catching fire than current Internal Combustions Cars (ICE) (Vesa Linja-aho 2020) (SAE J2990), especially from mechanical induced failures, the current battery designs seem to be mostly conservative with enough safety margins to cover the uncertainties always arising with new technological approaches. On the other hand current designs still may be based unnecessary over-dimensioning to account for still unquantified uncertainties. Here a large potential for future optimization in cost, weight and volume and therefor range is assumed. In order to use that potential, precise realistic requirements for design and testing are needed.

2.1 Battery Pack Design Regarding Mechanical Environments in Current BEV

The further new designs go beyond common industry standards, the more uncertainties need to be dealt with. As most new BEV battery designs still involve significant improvements, currently especially towards cost optimization and vehicle range performance, a lot of new assumptions need to be justified and later substantiated. Typically, performance and safety testing are not only done on the full product level (in this case a complete real life production car) but taken down to lower component

Quick Response Code	Access this article online	
	Website: www.jtin.com.my	DOI: 10.26480/jtin.02.2023.61.71

Cite The Article: Benedikt Plaumann (2023). Consideration of Damaging Frequency Ranges of Structural Excitation for Testing Large Battery Packs in Battery Electric Vehicles (BEV). *Journal of Technology & Innovation, 3(2): 61-71.*

level in the V-model (VDI/VDE 2206). This is happening at an earlier stage in the product development process. With this decomposition approach, the single components can be properly developed with derived local mechanical environment requirements and tested against these requirements (verification) long before a full car is produced for the first time. If all earlier verification steps worked out well, the final full car validation is less likely to produce significant iterations of reworking the design (VDI/VDE 2206). Therefore, component testing gives many benefits, such as faster design processes, less design iterations, less likely failures in final validation.

Because of the rather disruptive development step from ICE to BEV vibration testing standards are mainly derived from the ICE environments. In general practice, many test campaigns have been based on the ISO 16750-3 (ISO 16750-3) mechanical environmental test specifications so far. But over the past years many more testing specifications for BEV components in general or even specific to Battery Packs in BEV have come into practice, closing some gap of knowledge, but not all. A comprehensive older overview can be found in (Ruiz et al. 2018), a more recent one in (Kutka et al., 2018). Several contributions like (Hooper und Marco 2016; Hooper und Marco 2014) propose different testing profiles, mostly remaining under the ICE focused ISO 16750-3 test levels for components attached to the vehicle body. Here, different tests are described for components attached to the vehicle body or to unsprung masses like the wheel suspension, for example. For large battery packs or traction batteries weighting several hundreds of kilograms, this approach of "components attached to the body" does not work out well anymore (Kutka et al. 2018; Plaumann 2022). As the battery weights roughly as much as the pure vehicle chassis & body, the added mass of the battery significantly changes the structural dynamics of the combined vehicle and battery. Depending on the design of the Battery Pack different amounts of stiffness will be added to this multi-body-system. Some approaches like the BMW i3 and other earlier BEV designs use a very stiff battery pack being heavily protected from outside influences and mounted into the floor section of the vehicle frame. The use of internal modules in this block approach enables a rather simple exchange of single modules or even the complete battery in case of failure or progressed aging as well as a very rugged protection against impacts from the outside. Other, more recent approaches tagged under "cell2car" use a differential approach where small modules or even single cells are directly integrated into the car chassis, adding their mass locally and also interacting with their stiffness, see Figure 1. Generally, the cells need to be mounted securely to the next structural level like an encasing, a module pack structure or even structural floor elements in the cell2car approach. Often this is done by using heat conducting material used for battery cooling. The stress caused on the cells itself from global deformation of the vehicle chassis may be significantly different depending on the choice between an integral stiff box or a differential placement and local interaction as it is shown in (Plaumann 2022).

The most recent testing standard for BEV battery packs is the ISO 19453-6 (ISO 19453-6). For the given recommendations regarding mechanical environmental testing this standard further distinguishes between different sizes of the battery pack, its location in the car and the interaction between the vehicle body, chassis and the battery pack. Large, heavy floor batteries interacting with the vehicle are treated in category 3 of ISO 19453-6 regarding its shock and vibration testing requirements. The other categories describe environments for smaller batteries with less interaction between vehicle and battery, which are more or less based on the approach of a small component attached to a large vibration structure. In category 3, the large battery packs with significant interaction between battery and vehicle do not have generalized test level for the mechanical environment given. Instead, the standard indicates the need for "vehicle specific profiles and testing time" or "vehicle specific time signals" for testing. This contradicts the goals of a rapid V-model design process because no trustworthy design requirements and test levels are given on the general normative level.

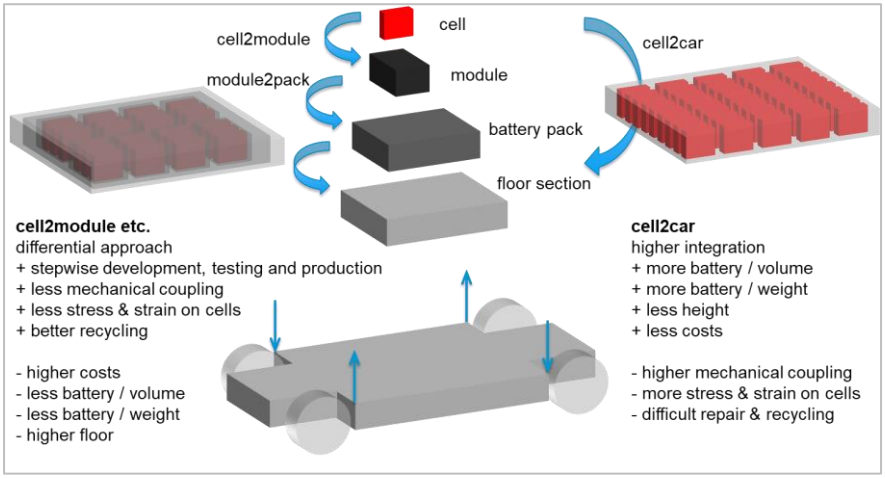

Figure 1: Different approaches of battery pack design, integral vs. differential in cell placement (Plaumann 2022)

Here further research is needed to derive partially generalized test levels and requirements depending on the stiffness/mass interaction between battery and vehicle frame. As current research indicates (Plaumann 2022), further research is particularly needed regarding a four-point-excitation test of a generalized large floor battery as in (ISO 19453-6), (Kutka et al., 2018; Dörnhöfer 2019). This is depicted by the blue arrows in Figure 2 later on, indicating independent movement of the battery pack corners in different directions at a given time step.

From a general point of view, all vibration testing specifications from standards and profiles from literature stated above describe a defined acceleration amplitude over frequency. In most cases the Power Spectral Density (PSD) of the acceleration environment at the interface joints to the Device Under Test (DUT), in this case the full battery pack. Sometimes a sine acceleration amplitude over frequency is also given. Shocks are often described in time-domain in most of the given standards. The main focus of this contribution lies on vibration testing, typically described mainly in frequency domain methods.

2.2 Frequency Ranges in The State of The Art

When describing movement or deformation of components, most vehicle simulation models from literature typically range up to 200Hz (Schramm et al. 2014). Movements of the suspension normally occur in the frequency region of 0,5 – 5 Hz. Typically structural dynamics testing schemes like (ISO 16750-3) use a frequency range of up to 2000Hz: This is done to cover potential local modes of small electrical components on circuit boards with potentially rather high resonance frequencies. This is particularly true for ICE excitations exhibiting significant acceleration input above 200Hz. For BEV Battery Packs the excitation mainly originates from the vehicle-ground interaction, often referred to as "road induced" (Hooper und Marco 2015). Any component in the transfer path after the suspension will see a mechanically low-pass filtered far-field spectrum, which is typically analysed up to 200Hz, see (ISO 19453-6; Hooper und Marco 2015; Hooper und Marco 2016).

A larger stiff Nickel Manganese Cobalt Oxide Pouch Cell showed resonance frequencies of around 200 Hz and 300 Hz, which is higher than typical road-induced vibrations of sprung masses in a passenger car. Internal vibration excitation may still originate from the electric motor but on a much smaller level than on an ICE.

2.3 Frequency Range Considerations for Test Setups

When defining, developing or choosing a suitable test setup for vibration testing, the following key figures of the vibration environment to be generated at the interfaces of the product need to be considered:

- maximum acceleration
- maximum velocity

- maximum deflection
- maximum force needed for moving the overall mass
- frequency range of application

The maximum force usually correlates to the theoretical maximum acceleration needed by simply applying Newton's Second Law. Resonance amplifications of the test setup and non-linear frequency behavior of needed electrical power over produced mechanical force of the test machine in use are the main points that need further thought on these two figures.

Maximum deflection, velocity and acceleration usually indicate the type of vibration test machine to be used. Typically, hydraulic shakers allow higher deflections, electro-dynamic shakers allow higher velocity and higher acceleration.

All physical descriptions of movement over time as well as the need force need to by described over the frequency range. This dependance of acceleration a, velocity v or deflection x over frequency is given by the following equations for ideal sine waveforms, here over time t.

$$x(t) = \hat{x} \cdot \sin(\omega t - \varphi)$$

$$v(t) = \hat{x} \cdot \omega \cdot \cos(\omega t - \varphi)$$

$$a(t) = -\hat{x} \cdot \omega^2 \cdot \sin(\omega t - \varphi)$$

The circular frequency ω can be transferred into the commonly used frequency f by $\omega = 2\pi f$. Any phase difference (if the sine wave doesn't "start" at 0) is given in the value φ. Peak values are denominated as $\hat{x}$ for the maximum deflection.

The influence of frequency on the correlation of acceleration and deflection can be shown when calculation the deflection of a typical sine weep using a constant peak acceleration of $\hat{a} = 10m/s^2$ (roughly $1g_n$) from 10 Hz to 2000Hz. Similar sine sweeps are often used for pre- and post-resonance searches of the vibration tests described above.

$$\frac{\hat{x}(10Hz)}{\hat{x}(2000Hz)} = \frac{2{,}5mm}{0{,}000063mm} = ca.\ 40.000$$

This very significant difference of displacement over a common vibration testing frequency sweep impacts on several issues for a good test result:

- choice of suitable measurement sensors, signal conditioning and data acquisition
- fixture design for a typically stiff, direct load transfer at the given interfaces
- test machine design or choice regarding machine resonances and guidance/bearing quality

Basically, the issues above describe several different impacts on the quality of the test regarding main test axis quality as well as unwanted cross-talk to another axis.

Therefore, the choice of a suitable frequency range impacts the technical implementation of a test and its costs as well as the achievable test quality.

2.4 Scope

This contribution presents a way of deriving a suitable frequency range for defining realistic vibration testing procedures for large BEV floor batteries.

The frequency range should cover any power distribution of the vibration environment to be tested necessary for achieving the test goals. As most tests on such large structures as complete battery packs usually include a strength and fatigue substantiation goal, the test frequency range should cover any vibration power contribution causing stress or fatigue-related faults on Battery Packs. Other test goals like substantiating maximum deflection/deformation requirements are typically closely correlated to the occurring stress for such components as a battery, where maximum deflection does not impair comfort, for example.

3. METHODS

3.1 Movements in Time-Domain

Rigid body movements of ground vehicles are widely described in literature, as i.e. (Schramm et al., 2014). In the case of a large traction battery mounted in the floor segment of a vehicle between the wheels, the excitation input is coming from the wheel suspensions where the interaction with the inertial forces of the complete vehicle happens, see Figure 2 with the vehicle coordinate system.

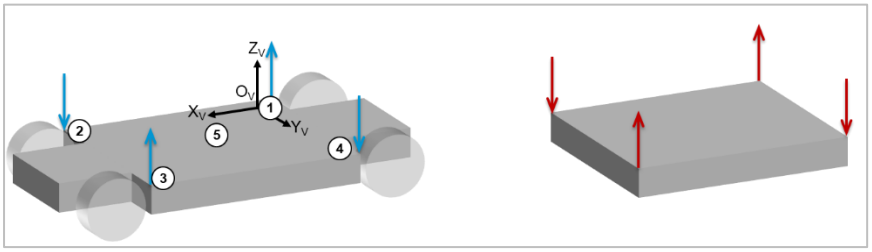

Figure 2: Incoherent movements (left) and incoherent excitation forces (right) on the corners (indicated by different directions) on a vehicle chassis (Plaumann 2022)

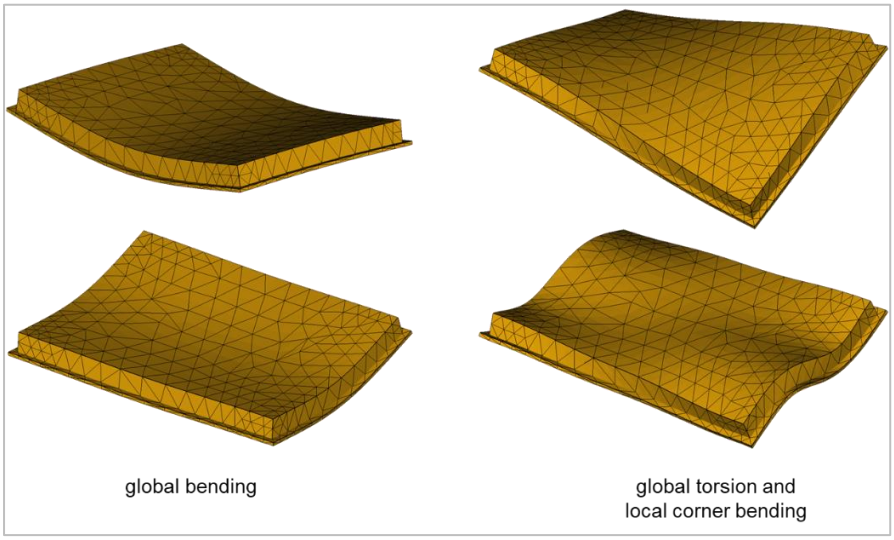

Figure 3: First two modes of global bending (left), simple mode of global torsion and local corner bending (right) for a vehicle floor battery pack, similar to (ISO 19453-6), see also (Plaumann 2022)

A description of general elastic deformation types of a simplified large traction battery in the floor segment of a vehicle body is described in Figure 3.

It is easily understandable that these deformations and movements cause local stresses and deformations in the battery structure and cells. The deformations are caused by inertial forces as well as incoherent forces acting on the corners. A more detailed description is given in (Plaumann, 2022).

Local and global resonances will amplify the deformation and induced stresses depending on the damping of the corresponding mode shape. This will increase the occurring stresses and deformations with excitations of the resonance frequencies, increasing the likelihood of fatigue failure by a large factor. Even though current electric vehicles do not fail more often than ICE vehicles (see (Heinzen et al., 2023) for more information), industry reports from battery pack component testing show a significant problem with leaks at the end of the testing series. Often the last test of the battery pack test series involves lowering a heated battery pack into cold water, testing for leaks under the imminent under-pressure inside, simulating for river-bed crossings of the vehicle. Leakage of water into the battery pack normally causes unwanted short-circuit reactions in the battery pack. It is assumed that testing with a four-poster corner excitation, which is not tested so far in current battery pack test standards, instead of the stiff platform single axis excitation used nowadays will increase stress and strain on sealing. Therefore, it is necessary to analyze the effect of corner excitation on battery pack reliability.

In order to describe the first relevant global and local corner bending mode shapes, the structure is described with translational movement vectors at five points, consisting of four corner and one point in the middle. For a first estimate the floor battery is considered as a continuous homogeneous structure in the vehicle chassis.

The model can be further reduced to vertical movements at the given points, especially for the small bending deflections and local deflections to be expected. All points have a given distance in the horizontal plane (X,Y) from each other. All points can make a vertical movement over time. So, at a given time step t each point will have always the same X and Y distance from each other (this simplification is only acceptable for small movements). But each point may have a different Z value.

3.2 Mechanical Fatigue in Battery Pack Structures

When looking at the maximum loads a product may suffer before failure, the ultimate static strength as well as fatigue behavior have to be considered. Most common engineering materials show a correlation of tolerable stress over number of occurring load cycles at this stress as depicted in Figure 4 with the blue line. This Wöhler diagram or S/N-curve depicts the tolerable stress over the corresponding number of load cycles, both in log scale.

High cycle fatigue behavior is tedious to measure as the needed high sample numbers for each measured stress level need to be cycled to a high cycle number, inducing very long testing time for some materials and lower stress levels.

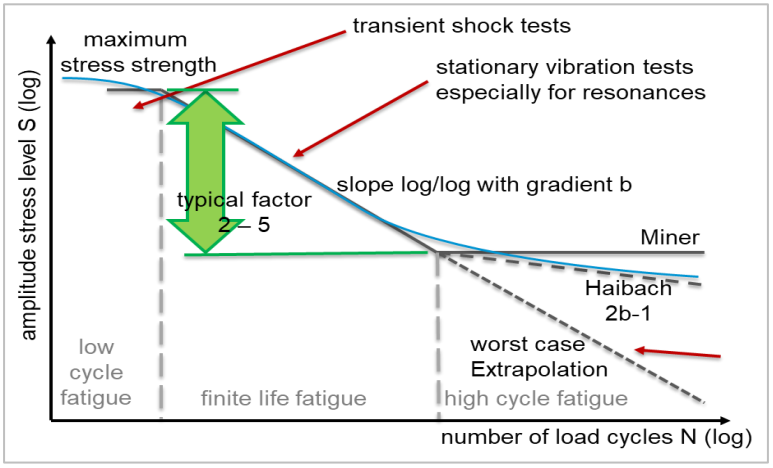

Figure 4: General Wöhler curve (SN curve) with used simplification, see also (Heinzen et al., 2023)

When multiple blocks of stress levels paired with their number of load cycles make up a load profile, the cumulative damage is calculated as follows, see also (MIL-Std-810G CN1). This is done by calculating the partial damage D_i at each occurring stress level by benchmarking the number of occurring load cycles $n_i$versus the tolerable number of load cyclesN_i, both at this stress level:

$$D_i = n_i/N_i$$

The whole damage is then

$$D = \sum D_i$$

Any damage $D \geq 1$ will lead to failure.

The slope of the SN-curve in log/log scale correlates how much high stress with only a few load cycles contribute to the overall damage of an excitation in comparison to many more load cycles at lower stress levels. The slope parameter b (basquin exponent), sometimes also referred to as k (ISO 16750-3) or m (MIL-Std-810G CN1), weights this influence over different stress levels and their load cycle numbers in an excitation. In typical fatigue analysis, the straight line will bend towards infinite or many more tolerable load cycles if the stress level remains below this durability stress level. In Palmgren-Miner, it is a horizontal line (below no failure will occur no matter how high the load cycle count), Haibach defines a certain decay by a new slop gradient, calculated by $2b - 1$.

Any description in the following will assume a worst-case behavior of a continuing gradient with no significant high cycle durability. This simplification allows the use of the slop without knowing the exact stress level at a certain point, where the critical failure of the whole product will start. This specific location and the corresponding stress level are often extremely difficult or even impossible to estimate correctly for a large product with many potential failure locations and miner production deviations. Therefore, a conservative approach of overestimating the high cycle damage is chosen to make the whole approach practical for application.

Most tests of large components like traction battery packs of BEVs focus on the substantiation regarding stress- or strain-based damage. In the following three different fatigue damage effects are considered:

1. The fatigue failure of metallic load carrying structures (potentially causing critical faults like short-circuits of mechanical damage to the cells) as well as

2. fatigue on electrical power and communication leads (potentially causing critical short circuit or malfunctioning of safety systems) need particular care in battery pack design and testing.

3. In addition to the leads, soldering in non-welded connections of power and data transfer circuits is considered with a particular focus on the solder itself, potentially causing the same critical short circuit or malfunctioning of safety systems as above for the leads

For reasons of lightweight design and good crash energy absorbing behavior, most of the load carrying structures of a large battery pack is made out of aluminum with welded connections, which are a particularly focus for fatigue analysis. From literature data a mean slope gradient of 5 is chosen for common aluminum structure (5XXX, 6XXX) with welded attachments and typical heat treatments from (EN 1999-1-3) as well as additional literature like (Haibach 2006) and (Dimitris Kosteas). This is a rather low gradient, already including some performance deterioration from manufacturing and imperfections. There are even lower potential values possible especially when considering defects. But lower gradients

will be covered farther onwards which is why a gradient of 5 is used for a good standard estimation of welded aluminum parts.

The behavior for copper leads is quite similar to the aluminum slope gradient, which is why the value of 5 is also used for the copper leads.

Quite different is the fatigue behavior found for typical solder connections. Here a slope gradient of 2 is taken from Wöhler-curves in (Shinohara und Yu 2010; Piet J.G. Schreurs 2002). The exact value may vary slightly for the real-life application of the battery packs, also because of the stress in the literature used is induced thermally and over a rather low number of cycles. But in general, the rather low value of 2 generates different results in the later FDS and can be used for defining differences in contrast to the aluminum structures with a slope gradient of 5. Depending on the soldering process and material even lower gradients may occur but here 2 is used a an already rather low value for this influence parameter study.

3.3 Choice on Velocity

For general simplification, not the exact stress level is chosen, but the measured or calculated dimension of movement as acceleration, velocity or deflection. As the scope in this contribution is the estimation of damage from vibration excitations on RESS in BEV, the governing occurring stress level in regard to the tolerable stress level at the point of failure would be a good choice. Unfortunately, the measurement of occurring stresses as well as the knowledge on their tolerable limit is very tedious to measure and calculate. For larger product this knowledge is nearly impossible to obtain at reasonable costs for all possible points of failure. Instead of the stress level, a simple measure of potential damage is calculated based on the velocity a resonating mass segment has, (McNeill 2008). The choice of velocity as a measure of potential damage is quite well established as (Gaberson 2012) describes. As described in this source, the link can be derived from $E_{kin} = m * v^2$ (Crandall 1962) or other as in (Gaberson and Chalmers 1969; Hunt 1960). The correlation of the occurring stress σ is described by multiplying the modal velocity v with a form factor K for the structure of interest, which describes the failure inducing peak stress to the mean stress i.e. for bending in a beam, the Elastic modulus E and the density ρ:

$$\sigma = K * \mathrm{v} * \sqrt{E * \rho}$$

Appendix A in even gives typical max-stress-to-failure of different materials transferred to a corresponding peak modal velocity (Gaberson 2012). It is also pointed out, that imperfections may increase the scaling factor K from its rather low theoretical value. Furthermore, it is all based on modal properties, where i.e. resonating mass m may only be a certain fraction of the total mass of the potential resonator of interest.

If not stress is primarily inducing failure but high deformations, leading to high strain rates, then the relative displacement between excitation and resonating mass segment may be chosen, see also (Ahlin 2006). This might a worth future considerations for large torsional deflections of battery packs where high strain may be more problematic than high stress in very yielding structural parts. But typically in these mechanical damage studies, the pseudo-velocity of the vibration system in resonance is a better assumption for the stress and hence induced damage contribution as given in the literature above.

3.4 Digital Filter for Time-Domain Response

The basic step to calculate the assumed response of a fictive worst-case vibration system with a resonance at each frequency step of the analysis is typically done by using digital filter. The measured signal, typically measured as acceleration at a given interface defines the mechanical environment to be replicated at this interface. If different waveform types are to be compared, the response analysis gives many advantages in addition to the common frequency domain analysis. For the analysis, two steps need to be carried out. First the response of the vibrating system need to be calculated. Then the acceleration response to the measured input acceleration needs to be transferred to the vibration velocity a system with a resonance at every frequency point. A well standardized way to calculate the movement of a worst-case fictive vibration system is the use of digital filters. In the case of this contribution these filters can also be used to calculate the response or the resulting movement of the fictive system in another dimension than the acceleration, i.e. the velocity of the vibration system excited by the given measured acceleration signal. This is described in (ISO 18431-4).

The digital filter uses a Laplace transformation of the input system to the calculated output of the system for each frequency step. It is assumed that the worst-case vibration system has a resonance of a single-degree-of-freedom (SDOF) system at each frequency step in the analysis. For this contribution the analysis used a rather broad frequency segmentation of a frequency step each 1/6th of an octave. This coarse analysis approach is not as critical as in a Fourier Transform, where distinct tones in a frequency range may be omitted or smeared by a rather broad frequency resolution. In our case we typically look a rather broad resonance behavior (low damping) of the resonating system. So the critical resonance would still be significantly excited even with a tonal excitation at a slightly different frequency. The ISO 18432-4 describes different digital filters to calculate relative-velocity and relative-displacement responses from the given signal (relative movement between excitation and the resonating mass) as well as pseudo-velocity and pseudo-displacement of the resonating mass. Also, the absolute acceleration response of the vibration mass excited by the input acceleration can be calculated using digital filters. Here, we use pseudo-velocity responses because of its good relation to induced stresses.

3.5 Shock Response Spectrum

A typical Shock Response Spectrum (SRS) would then be calculated by looping through all SDOF responses (for each frequency step) and checking the absolute maximum response. That single maximum value of global minimum or maximum (called maximax) is then taken for the value in the plot for the resonance frequency of the current SDOF-system.

As only the single maximum of each response is taken, the SRS will not change for longer measurement signals as long as no further new maximax response arise from the further excitation. The SRS is therefore only depending on the maximum, making it perfect for analyzing and comparing shocks.

3.6 Fatigue Damage Spectrum

The Fatigue Damage Spectrum (FDS) is using a different analysis of the time-domain responses coming from the same digital filters as above.

Here, the induced damage is of interest. As damage contribution depends on the level of the velocity and its corresponding number of load cycles, all "weighted" by using the slope of the Wöhler-curve as an exponent for the stress level, here assumed to be proportional to our velocity level. For this, a histogram of each SDOF-response is calculated by an appropriate method of classification. Rainflow-counting is a very powerful tool but other methods as level crossing may also yield similar results in the later FDS. The counting method gives a histogram of velocity levels and its corresponding number of load cycles for each SDOF-response. As only the peak values of each cycle are of interest, the single contribution count must be used for level crossing, not the cumulative level crossing. Other counting methods provide a single contribution count directly. The process is depicted in Figure 5 for a measured acceleration excitation on the right front axle.

The simplified analysis in this figure uses a fictive vibration system with five distinct resonator frequencies, each damped with 5% damping ratio. The pseudo-velocity responses of the fictive system (assumed to be proportional to stresses) are calculated by digital filters. Then, the calculated velocity responses of the resonating masses are each transferred into a histogram using level crossing counting on a rainflow matrix of closed cycles. The single contribution level crossing classes (only peak values of closed cycles) now have a corresponding cycle count. The pseudo-velocity values of each class level are then exponentiated by the weighting exponent derived from the slope of the Wöhler-Curve (in this simple case exponent 2). Finally, all exponentiated velocity values are multiplied by its corresponding count number and summed up to form the damage contribution of the actual resonator at its resonance frequency.

As a general remark on the comparability of absolute damage calculations, many scaling factors of the result must be clearly given along with the calculation result. This includes:

- Units of input and response (m/s^2 is better for input than gn, as the later one can be easily transferred to pseudo-velocity in m/s)
- Damping ration of resonators at each frequency.
- Type of calculated response (here pseudo-velocity, given in m/s)
- If needed: Correlation factor from pseudo-velocity to induced stress level, so that it can be compared to tolerable stress levels. Otherwise, the damage is just a proportional damage index or must be benchmarked to the bearable damage velocity count.
- Type of counting method for the histogram (may yield slightly different results, depending on the signal analyzed)
- Slope of the assumed Wöhler-curve used as weighting exponential factor

The limitations of this approach include the following points:

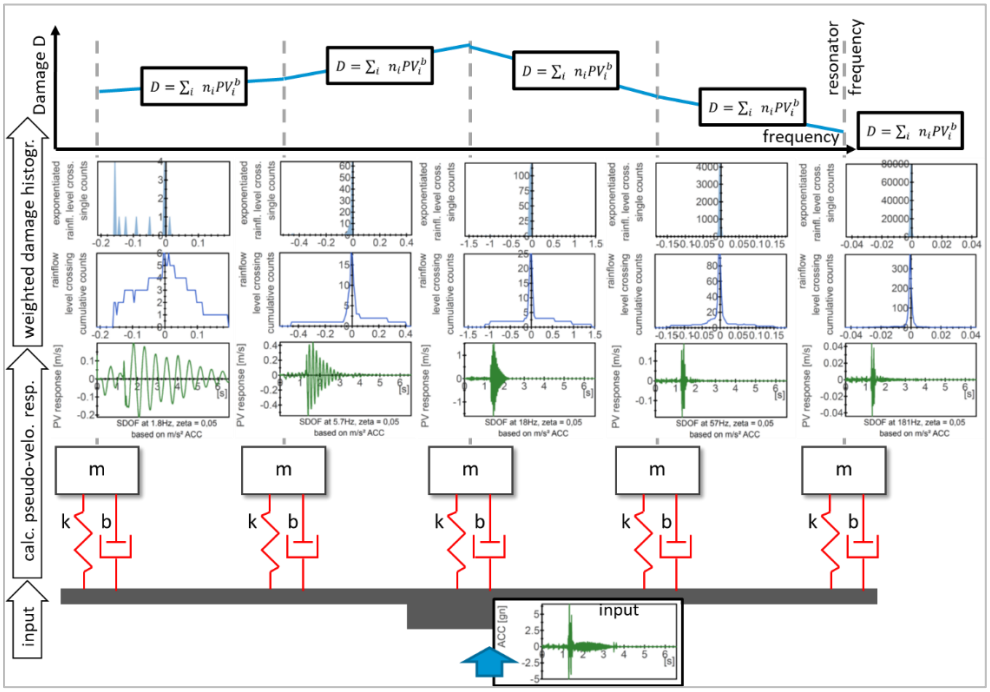

Figure 5: Process of Fatigue Damage Spectrum Calculation for 5 SDOF-frequency points, each for pseudo-velocity response of a 5% damped resonator for a real excitation signal acceleration input

3.6.1 Over-Estimation in Frequency Regions of No Resonance

The estimation using a vibration system with a resonance at each frequency point may yield unrealistic high damage values in frequency ranges where surely no resonance will be. In the case of the battery with first global and most local resonances start above 10Hz, any assumed resonance under 10Hz will give far too conservative damage contributions. This could be solved by using a non-constant damping factor of the frequency range reducing amplifications from resonances to near 1 below 10Hz. As for reasons of comparability a constant factor of 10 (5% damping ration) is used over all frequencies, the damage estimation gives values being too high by the factor of up to 10^b. Therefore, we will later not consider values below 10Hz where we know that no resonance exists.

3.6.2 Over-Estimation of Stress-Levels in The Infinite-Life-Range

Many engineering materials have a factor of 2-4 between ultimate maximum allowable stress levels for short-time life (upper left region in Figure 4) over the level of assumed infinite-life (bottom right region in Figure 4) or long-term-fatigue. Typically, any stress value smaller than factor 5 by the highest value in the test series of consideration is neglected as being irrelevant in fatigue analysis. If a certain potential damage does not occur under the maximum stress level induced in the test level, all values small than $1/5^{th}$ of this values don't need to considered for finite-life fatigue analysis. The SRS is used to estimate the corresponding maximum stress from each measurement data set by its corresponding maximum pseudo-velocity value.

3.6.3 Measurement Length

The FDS in contrast to the SRS is highly sensitive to the length of the measurement signal, as each zero crossing cycle will add more counts to the histogram. An SRS uses only the highest maximum or lowest minimum of the complete data series considered. Measured data sets need to be long enough with enough data points as to get rid of statistical influences from too small data sets. For better comparability, all FDS plots are scaled to an assumed exposure duration of 1h. Other durations can be easily calculated by linear multiplication as the number of load cycles n does not go under the exponent b, see Figure 5.

3.6.4 Measurement Campaigns

This analysis is based on the first results of a smaller pre-test measurement campaign, with more planned in the future. These current results indicate significant changes on the approach compared to the state of the art of component vibration testing. The later following novel analysis to derive information on the frequency range to be considered for testing uses mainly the same original set of data as in (Plaumann 2022). There however, the focus only remains on significant transfer functions.

3.6.5 Real World Excitation on Different Surfaces And Events

The data for analysis was measured on serial production cars in real world environments on different road surfaces under varied loading configurations. Each measurement is defined by vehicle, road surface, loading configuration and repetition. The road surfaces include but are not limited to: pot hole - 30kph, cobble stone - 30kph, gully - 30kph, city drive HH - various speeds, country road - 100kph, motorway - 130kph, country roads - various speeds, rough cobble stone - 30kph. Furthermore, the noise floor was measured.

3.6.6 Vehicles

The following preliminary analysis uses mostly the data from measurement on a VW ID3 as shown Table 1 with the most relevant technical data.

The preliminary data set also contains data of measurements on VW T5 and BMW i3. Due to the generality of the approach presented here, the following analysis shows mostly the data from the VW ID3 measurements for comparison in different road surface events. The table shows empty and max gross weight of the vehicles as well as information on the additional loading in the measurement campaign. Beside the mass loading of the driver and minor other masses, the additional masses loaded are given in the table.

Table 1: Vehicles Used for the Preliminary Analysis

vehicle	Compact BEV VW ID3	Compact BEV BMW i3
empty weight	1810 kg	1320 kg
max gross weight	2270 kg	1670 kg
added mass loading to driver etc. (80kg)	200 kg	87.5 kg 162.5 kg
battery energy	62 kWh	33 kWh

3.6.7 Measurement Equipment and Signal Quality

The measurement and data acquisition equipment used is described in Table 2.

IEPE one-axial piezo accelerometer with charge amplifiers PCB M353B18 +/- 500gn at 10mV/gn PCB-483C05 AC coupling with constant current for charge amplifiers
USB data acquisition system Meilhaus Redlab, rebranded Measurement Computing (MCC) 1608G with 16bit, 16 analog inputs at +/- 1 to 10V, 250kS/s common rate sampling rate per channel 15kHz

Further signal checks were performed based on the comparison of RMS versus standard deviation (mean offset), high kurtosis or high skewness values (impacting or contact losses) as well as general possible data errors. Questionable data was not used for analysis.

3.7 Analysis Software

Most of the analysis is done with National Instruments DIADEM 2020. This includes digital filtering, frequency domain compensation, Fast Fourier Transformation (FFT), Power Spectral Densities (PSD), transfer functions with amplitude and unwrapped phase, coherence functions, Cross Spectral Densities (CSD), channel arithmetic for time domain difference functions, statistical distributions (random probe) and statistical key figures like Root Mean Square (RMS), min, max, kurtosis and skewness.

The digital filter responses were calculated using the VB-Scripting interface of DIADEM based on the filter algorithms of ISO 18432-4 and verified to other industry implementation as well as examples from the literature given above.

4. Results

As described earlier on, many important boundary conditions for the correct testing setup depend on the frequency range of interest for the scope of the test. Most tests of large components like traction battery packs of BEVs focus on the substantiation regarding stress- or strain-based damage. The fatigue failure of metal load carrying structures (potentially causing critical faults like short-circuits of mechanical damage to the cells) as well as fatigue on electrical power and communication leads (potentially causing critical short circuit or malfunctioning of safety systems) need particular care in battery pack design and testing. Therefore, this contribution looks at the pseudo-velocity shock response regarding their potential damage using the fatigue damage spectrum.

The analysis of the electrical power and information transmission further distinguishes between the actual copper leads process for power of communication transmission (which has a similar fatigue exponent as welded aluminum) as well as actual solder used to connect two copper parts (having a different exponent).

As shown in similar publications (Plaumann 2022), two different basic dynamic load cases of the large floor-mounted battery packs needs to be considered:

- torsion of the pack, mostly together with local corner bending under different vertical movement of the four corners
- global bending, especially in resonances

Obviously, the exact exponents of the Wöhler-curve assumed for the following analysis may differ depending on the exact type of aluminum, the type of welding, the type of crack initiation and the heat treatment used on the metal. Generally, a higher exponent will "rotate the resulting FDS plot clockwise" at small acceleration levels towards a steeper downwards line at higher frequencies and vice versa. But from the comparison of the two choices under consideration in the following, as feasible result on the scope of the contribution can be reached.

The events considered for analysis are:

- transient shocks from driving over a manhole cover
- a rather common cobble stone path
- a very rough cobble stone path

The resulting damage is calculated for a repetition of each measured event as to amount to 1h of testing time. Damping of the shock response worst case fictive system is set to 5%, corresponding to a quality factor or amplification of 10. The scaling from pseudo-velocity to stress is set to 1, making the numbers in the plot not directly readable in N/mm^2. Therefore, the vertical axis is denominated as an "index" proportional to the stress damage induced.

4.1 Fatigue Damage on Welded Aluminum and Copper Leads

A potentially critical failure mechanism in mechanical load-bearing structures of large floor mounted battery packs is the failure under stress concentration in a welding of the mostly aluminum structure. Therefore, this will be analyzed first.

The exponent of the Wöhler-curve for welded aluminum is assumed to be near 5. A similar exponent of the Wöhler-curve is typically used for copper leads processed for power leads and communication wires. Therefore, this analysis covers both potential failures.

Forced corner bending b=5

We start with the forced corner bending and torsional effects, mostly related to the different input from the suspension to the four corners of the pack. Depicted in Figure 6 is the fatigue damage spectrum for the measurement of the right front (RF) measurement point on the battery for three different driving events.

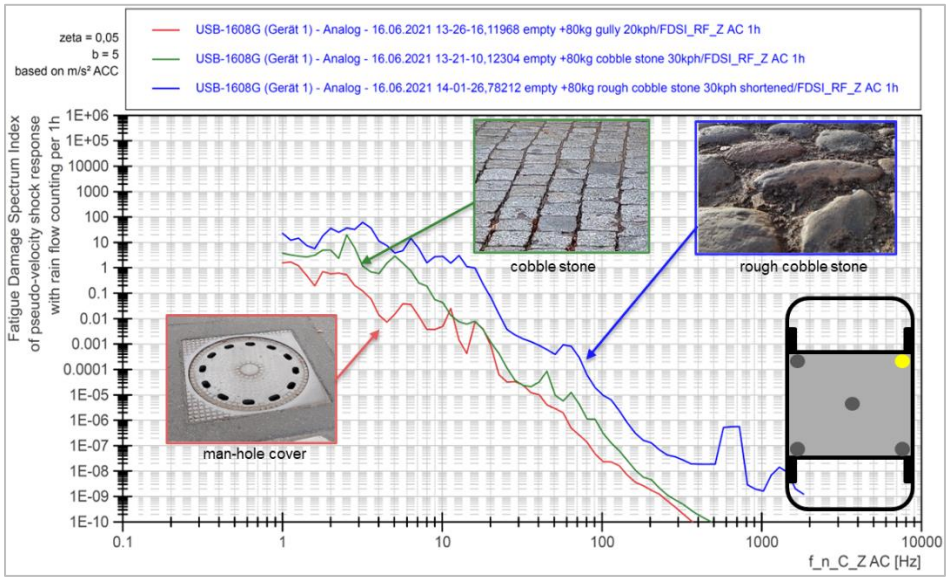

Figure 6: FDS of the right rear (RF) corner of the battery pack with Wöhler-curve exponent of 5 and 5% damping. (Heinzen et al. 2023)

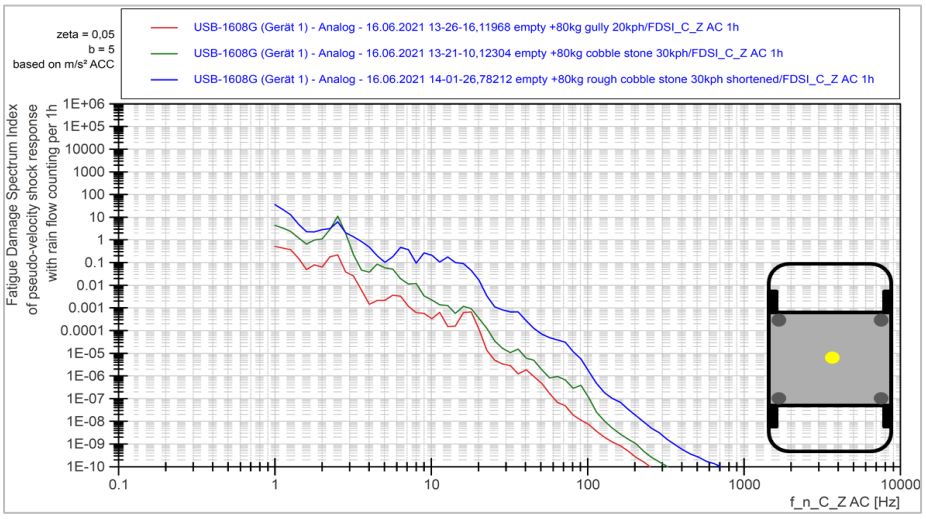

Figure 7: FDS of the midpoint of the battery pack with Wöhler-curve exponent of 5 and 5% damping.

The Figure 6 shows a rather steep decay of the resulting damage over frequency the higher the potential resonance frequency may be as well a high damage contribution between 1 and 10Hz. The contribution of any frequency above 20Hz is more than four decades lower than the contribution of up to 10Hz. This is similar over all three events with different absolute damage levels. As expected, 1h of driving over rough cobble stone generates higher damage than driving over smoother cobble stone. The manhole cover shocks are not occurring often enough to amount to similar levels than on the rough cobble stone track.

When looking at global bending damage in resonances, Figure 7 also indicates a steep decay but with the most significant damage contribution having moved to even lower frequencies below 5Hz. As described above, the damage will be highly over-estimated below 10 Hz as no resonance frequency will occur.

The additional mass and interface contacts along the transfer path form the corner to the middle may have reduced the damage contribution of higher frequencies even further.

4.2 Fatigue Damage on Soldered Interfaces

As solder itself is also a prime potential failure mechanism in electrical power or information transmission, the following analysis will focus on this, using a different exponent of the Wöhler-curve for solder: 2.

4.2.1 Forced Corner Bending

Displayed in Figure 8 is the Fatigue Damage Spectrum for the right rear (RR) point of the battery with every parameter the same as in Figure 6 except for the different exponent (here 2 instead of 5). This is used to look a forced corner bending and torsional effects.

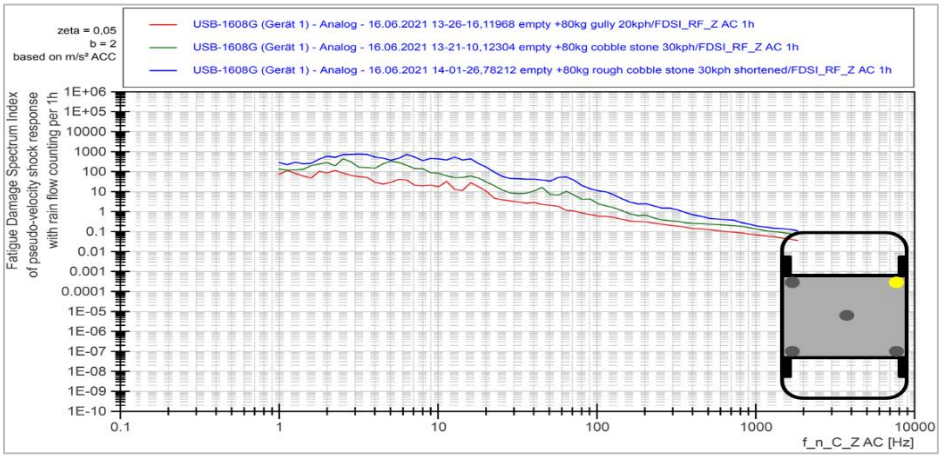

Figure 8: FDS of the right front (RF) corner of the battery pack with Wöhler-curve exponent of 2 and 5% damping.

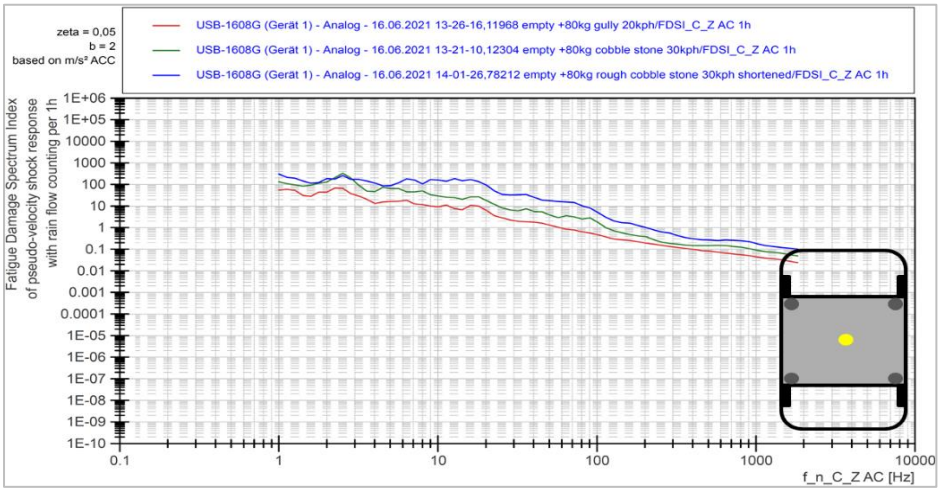

Figure 9: FDS of the midpoint of the battery pack with Wöhler-curve exponent of 2 and 5% damping.

The slope appears rotated upwards (counter-clockwise), meaning that higher frequencies contribute more the absolute damage in the considered failure mechanism. Only the damage contributions of the frequencies above 200Hz are three decades lower than the damage of up to 20Hz.

The global bending shows a similar damage contribution, as seen in Figure 9.

In contrast, Figure 10 depicts the Fatigue Damage Spectrum of the measured accelerations in the vicinity of the right front axle. These unsprung masses typically show significantly higher acceleration levels, especially at higher frequency levels than the vehicle body as long as engine vibrations are not too dominant. The plot is based on an exponent of 5, typically describing the fatigue of joined light metal structures quite well. Pure steel structures may have slightly different exponents.

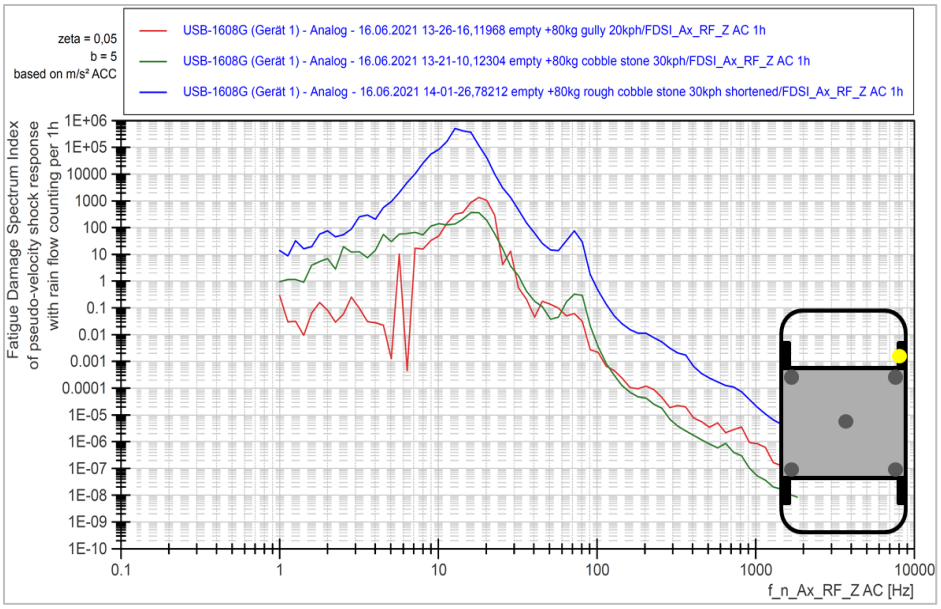

Figure 10: FDS of BEV right front axle (unsprung masses) with Wöhler-curve exponent of 5 and 5% damping.

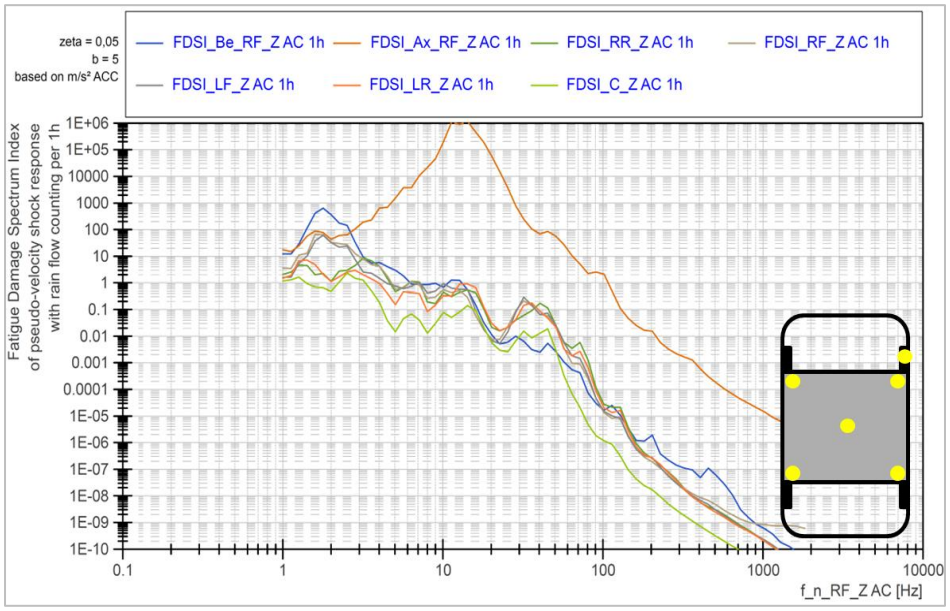

Figure 11: FDS of all points measured with Wöhler-curve exponent of 5 and 5% damping for rough cobble stone.

The effect of the low-pass characteristic of the suspension can be clearly seen in comparison of Figure 10 to a corner FDS as in Figure 6. The damaging influence of higher frequencies has been filtered out by the suspension.

When looking all al measurement points considered here for the BMW i3 under the rough cobble stone road induced vibrations the results derived above seem to be replicated very well, too. This can be seen in Figure 11.

4.2.2 General Remarks

As in most fatigue analysis approaches, the exponent b, which "weights" the damage induced at high levels and low cycle counts over lower levels with higher counts, is of crucial interest. The lower the exponent b, the more the Fatigue Damage Spectrum (FDS) plots are turned counter-clockwise with the higher frequencies coming up. When looking at the question of damaging contributions over frequency to be covered in battery testing, this leads to the generalized results, that especially fatigue failure mechanisms with lower exponents b increase the damage influence of higher frequencies. The low exponents of b occur i.e. for lightweight materials with imperfect welding, many pre-initiated cracks etc. Also, the fatigue behavior of solder with quite low cycle counts found in the given literature falls into the category of rather low values of the exponent b, all coming from a rather steeply falling slope in the Wöhler-curve. Here, a rather low exponent of 2 proposes a worst-case scenario of potential fatigue mechanisms for damaging frequency contributions.

Considerations regarding the frequency range for future vibration component testing of large battery packs. As described in (Plaumann 2022, ; ISO 19453-6) the vibration testing of large battery packs need to be reconsidered as the typical approach with treating the component under testing as an attachment to a larger part is not valid for large, heavy battery packs interacting significantly with the rest of the vehicle.

For the given example of vibrations on the floor-mounted battery in a VW ID3 and correspondingly the BMW i3 it can be seen that the four corners have slightly higher ranging damaging frequency bands than the middle of the battery pack. This may be explained by the large mass fractions of the battery in the load path from the force-excited corners to the middle of the battery.

The main calculated damage contribution lies around 3Hz for welded aluminum or structures with a fatigue slope of 5 at the corners and lower frequencies for the middle. For a worst-case assumption of even lower exponents (as for example 2 for solder used in this analysis) the damaging frequency content is ranging up to 20Hz. Regarding the potential damage at low frequencies, it must be noted that the high damage contribution of the plots is based on a worst-case assumption that the corresponding SDOF resonator does resonate at these low frequencies. It can be seen in similar publications that in real BEV Battery Packs or similar structures resonances occur only at frequencies higher that at least 10Hz (Altmann et al., 2021; Plaumann). Therefore, the fictive resonating system of the FDS assumes a potential damage from a resonance that does not occur in real vehicle structures of interest here because it assumes an amplification of up to factor 10 in resonances that don't exist in reality. Only the highly damped suspension frequency would fall in that really low frequency range. But this does not matter when looking at the battery behind the suspension in the load path. Therefore, the following analysis considers only damages above 10Hz. Normally the peak damage values considered then occur in the region of 10 - 20Hz leaving out the unrealistic high calculations below 10Hz.

Looking at the upper frequency region, a reasonable upper frequency cut-off for battery component testing would be at around 200Hz-500Hz, especially for low fatigue exponents. The damage contribution of frequencies higher than 200Hz is three or more decades lower than the main contribution frequency band of up to 20Hz. For the future justification, a look at infinite life of very high cycle fatigue is need to establish a what threshold damages will not be counted anymore because they are so small that they fall in infinite-life-fatigue. An estimation of the upper and lower bond of the falling SN-curve with short time fatigue and infinite-life fatigue boundaries is shown in based on the shock response spectrum (SRS) (Heinzen et al., 2023). Even though we look at more or less stationary excitations, the maxi-max analysis of the stress-correlating pseudo-velocities give an indication at what stress levels the contribution does not contribute further to the overall damage. The Fatigue Damage Spectrum (FDS) plots shown here do not help much finding the infinite-life threshold because the FDS is weighted by the fatigue exponent b and is averaged over the measurement. The SRS will give the maximum value that is relevant for describing the upper and lower boundaries to be considered for infinite-life-considerations. Together with the work in an upper threshold of 200 Hz to 500 Hz depending on SN-curve exponents, vehicle and road surface can also be established (Heinzen et al., 2023). Future measurements will need to substantiate that on a broader base of measurements for different vehicles and road surfaces.

The unsprung masses of the wheel axle assembly show even higher ranging damaging frequency bands but are not considered here any further. When transferring these results into requirements for future vibration testing of large BEV batteries, then the frequency range between 3 and 200Hz needs an adequate replication of the potentially induced damage. This rules out any non-linear contact impulses (coming for example linear bearings) at least of up to 500Hz to be able to replicate the correct induced damage under all loading conditions. Any high frequency non-linear "rattling" generally induces high-kurtosis leading to higher damage than typical sine-waveforms. This may also be the case for servo-hydraulic shaker valves with non-sine waveforms at frequencies near the maximum switching frequency. This could cause induced damages in the test that do not occur in real-world excitations. Electro-dynamic (ED) shakers can easily generate high frequency excitation replication of up to 500Hz with rather high signal quality (Piersol et al., 2010; Ben Haest 2014).

Regarding the potential replication of these damage contributions in vibration testing, servo-hydraulic shakers generally offer much more deflection for rather severe low frequency excitation than most electrodynamic shakers, (Piersol et al., 2010; Ben Haest 2014). Generally, most test specifications work well on ED shakers from above 5Hz onwards. As long as the tested batteries do not have resonances below that range, an ED shaker neglecting the frequency range between 1-5Hz or even 1-10Hz would still cover the relevant frequency range inducing damage from the beginning first resonance frequency of the battery upwards up to maybe 200Hz. A good signal quality should be further kept up to maybe 500Hz as not to inflict unwanted damage. Any excitation above that frequency would most likely do not cause any further notable damage because the FDS has gone down so many decades that even if the battery has resonances there, the corresponding damage is neglectable.

5. Limitations of the Study

This early analysis of a pre-test measurement campaign is based only on measurements of one BEV. Therefore, the results cannot be generalized regarding the given quantitative information. So far, the effects found relevant for future testing requirements can be only generalized on a qualitative or rather broad quantitative scale. A quantifiable analysis of a broader data base will yield more robust results. Therefore, no PSD plots for potential random vibration testing environments are given in this contribution as more test results are needed to derive a proper test specification regarding vehicle life and fatigue damage effects.

However, the process described here will remain the same when applied to a broader set of measurements in the future. As this will be a long and continuously running task for OEM, suppliers or academia in the upcoming intense phase of design and verification of new BEVs over the next years, the findings described here can be considered in the specification of adequate test setups.

Even though the use of pseudo-velocities to estimate proportional mechanical stresses for failure estimation is the usual approach commonly considered best, it is a question whether high torsional deflections causing potential damage from large strain effects should be reflected rather by relative-deflection than pseudo-velocity. On the other hand, the torsional deflections are not considered to be so large that high strain failure is likely.

6. Conclusion

The analysis of some pre-study measurements has shown a reasonable and practical way to estimate the frequency range in which relevant damage may occur in battery packs. It was also shown that the frequency range estimation highly depends on the material properties considered to be a potential failure, the road surface and the vehicle. But it can also be shown from the rather small set of data analyzed that the upper frequency range to be considered is at least 200 Hz, potentially rather 500 Hz, especially when looking at delicate failure in soldered connections.

Based on the data set of this preliminary test campaign it can be assumed that electrodynamic shakers may be needed to enable a realistic damage replication for electrical components in a battery pack with soldered interfaces. Servo-hydraulic shakers with a limited frequency range of non-disturbed excitation will likely excite frequency ranges that are only causing damage in mechanical parts, hence replicate not all potentially relevant failures in battery packs. It must be noted that for definite frequency range recommendation in vibration testing of large battery packs further measurements are needed.

Funding Statement

The author received no specific funding for this pre-study. There are pending funding proposals for the further progress of the path described.

Conflicts of Interest

The author declares that he has no conflicts of interest to report regarding the present study. The author has worked and been involved in the developed both in labs focused on hydraulic shakers as well as labs focused on electrodynamic shakers over his career.

References

Ahlin, Kjell, 2006. Comparison of test specifications and measured field data. In: Sound and Vibration (September 2006), Pp. 22–24. Online verfügbar unter http://www.sandv.com/downloads/0609ahli.pdf.

Altmann, M., Kotter, P., Seifert, J., 2021. Auswirkung von Betriebszuständen auf die Mechanik von Lithium-Ionen Speichersystemen – Anforderung und Absicherung. In: N. Schmudde (Hg.): Workshop Brennstoffzelle, Batterie, elektrischer Antrieb – Anforderungen und Absicherung. Workshop Brennstoffzelle, Batterie, elektrischer Antrieb – Anforderungen und Absicherung. Ulm. DVM Deutscher Verband für Materialforschung und -prüfung e.V.: DVM.

Ben Haest, 2014. Good Vibrations: Quality Electronics Design S.A.

Dimitris Kosteas, 1999. Fatigue of aluminum structures EN 1999-1-3. Eurocode 9: Design of aluminum structures. TNO.

Dörnhöfer, Andreas, 2019. Betriebsfestigkeitsanalyse elektrifizierter Fahrzeuge (Fatigue analysis of electric vehicles). Berlin, Heidelberg: Springer Berlin Heidelberg.

EN 1999-1-3, 08/2011: EN 1999-1-3 Eurocode 9: Design of aluminium structures - Part 1-3: Structures susceptible to fatigue.

Hunt, F.V., 1960. Stress and Strain Limits on the Attainable Velocity in Mechanical Vibration. In: Journal of the Acoustical Society of America, 32 (9), Pp. 1123–1128.

Gaberson, H.A., Chalmers, R.H., 1969. Modal Velocity as a Criterion of Shock Severity. In: Shock and Vibration Bulletin, 40 (Part 2), Pp. 31–49.

Haibach, Erwin, 2006. Betriebsfestigkeit (Finite Life Fatigue). Verfahren und Daten zur Bauteilberechnung. 3., korrigierte und ergänzte Auflage. Berlin: Springer (VDI-Buch). Online verfügbar unter http://deposit.dnb.de/cgi-bin/dokserv?id=2710327&prov=M&dok_var=1&dok_ext=htm.

Heinzen, Till; Plaumann, Benedikt; Kaatz, Marcus, 2023. Influences on Vibration Load Testing Levels for BEV Automotive Battery Packs. In: Vehicles, 5 (2), Pp. 446–463. DOI: 10.3390/vehicles5020025.

Hooper, J.M., Marco, J., 2016. Defining a Representative Vibration Durability Test for Electric Vehicle (EV) Rechargeable Energy Storage Systems (RESS). In: WEVJ, 8 (2), Pp. 327–338. DOI: 10.3390/wevj8020327.

Hooper, James Michael; Marco, James, 2014. Characterising the in-vehicle vibration inputs to the high voltage battery of an electric vehicle. In: Journal of Power Sources, 245, Pp. 510–519. DOI: 10.1016/j.jpowsour.2013.06.150.

Hooper, James Michael; Marco, James, 2015. Experimental modal analysis of lithium-ion pouch cells. In: Journal of Power Sources, 285, Pp. 247–259. DOI: 10.1016/j.jpowsour.2015.03.098.

Howard A. Gaberson, 2012. Shock Severity Estimation. In: Sound and Vibration, Pp. 12–19.

ISO 16750-3, 15.12.2012: ISO 16750-3 - Road vehicles - Environmental conditions and testing for electrical and electronic equipment - Part 3: Mechanical Loads.

ISO 18431-4, 01.02.2007: ISO 18431-4: Mechanical vibration and shock - Signal processing - Part 4: Shock-response spectrum analysis.

ISO 19453-6, 07/2020: ISO 19453-6 - Road vehicles - environmental conditions and testing for electrical and electronic equipment - Part 6; Traction battery packs and systems.

Kutka, H., Müller, C., Fülöp, T., Dörnhöfer, A., 2018. Multilevel fatigue analysis of RESS in BEV/HEV - Multilevel-Festigkeitsentwicklungen der HV-Speicher von BEV/HEV-Fahrzeugen. In: M. Brune (Hg.): Berichtsband zur 45. Tagung des DVM-Arbeitskreises Betriebsfestigkeit. 45. Tagung des DVM-Arbeitskreises Betriebsfestigkeit. Renningen. Deutscher Verband für Materialforschung und -prüfung e.V. (145), Pp. 1–18.

MIL-Std-810G CN1, 15.04.2014: MIL-Std-810G CN1 Environmental engineering considerations and laboratory tests.

Piersol, Allan, G., Paez, Thomas L., Harris, Cyril, M., 2010. Harris' shock and vibration handbook. 6th ed. New York: McGraw-Hill Professional; London: McGraw-Hill [distributor].

Piet, J.G. Schreurs, 2002. Fatigue damage in solder joints. In: H.A. Mang, F.G. Rammerstorfer, J. Eberhardsteiner (Hg.): Fifth World Congress on Computational Mechanics. Fifth World Congress on Computational Mechanics. Vienna, Austria, July 7–12.

Plaumann, Benedikt, Anforderungen an die Vibrationsprüfung von großen unterflurmontierten Batterien für batteriebetriebene Elektrofahrzeuge (BEV) - Requirements for vibration testing of large underfloor-mounted battery for Battery Electric Vehicles (BEV). In: DVM Wissen. Online verfügbar unter https://dvm-wissen.de/de/brennstoffzelle-batterie-elektrischer-antrieb-anforderungen-und-absicherung/104-anforderungen-an-die-vibrationspruefung-von-grossen-unterflurmontierten-batterien-fuer-batteriebetriebene-elektrofahrzeuge-bev.html?q=Kategorien-Brennstoffzelle,+Batterie,+elektrischer+Antrieb+\-+Anforderungen+und+Absicherung.

Plaumann, Benedikt, 2022. Towards Realistic Vibration Testing of Large Floor Batteries for Battery Electric Vehicles (BEV). In: Sound and Vibration Vol.56 (No.1). DOI: 10.32604/sv.2022.018634.

Ruiz, V., Pfrang, A., Kriston, A., Omar, N., van den Bossche, P., Boon-Brett, L., 2018. A review of international abuse testing standards and regulations for lithium-ion batteries in electric and hybrid electric vehicles. In: Renewable and Sustainable Energy Reviews 81, Pp. 1427–1452. DOI: 10.1016/j.rser.2017.05.195.

Crandall, S.H., 1962. Relation between Strain and Velocity in Resonant Vibration. In: ournal of the Acoustical Society of America, 34 (9), Pp. 1960–1961.

SAE J2990, 07/2019: SAE J2990 - Hybrid and EV First and Second Responder Recommended Practice.

Schramm, Dieter; Hiller, Manfred; Bardini, Roberto, 2014. Vehicle Dynamics. Modeling and Simulation. Berlin, Heidelberg: Springer Berlin Heidelberg; Imprint; Springer.

Scot I. McNeill, 2008. Implementing the Fatigue Damage Spectrum and Fatigue Damage Equivalent Vibration Testing. In: Shock and Vibration Symposium.

Shinohara, Kazunori; Yu, Qiang, 2010. Evaluation of Fatigue Life of Semiconductor Power Device by Power Cycle Test and Thermal Cycle Test Using Finite Element Analysis. In: ENG 02 (12), Pp. 1006–1018. DOI: 10.4236/eng.2010.212127.

Sun, Peiyi, Bisschop, Roeland, Niu, Huichang, Huang, Xinyan, 2020. A Review of Battery Fires in Electric Vehicles. In: Fire Technol., 56 (4), Pp. 1361–1410. DOI: 10.1007/s10694-019-00944-3.

VDI/VDE 2206, 09/2020: VDI/VDE 2206 - Development of cyber-physical mechatronic systems (CPMS) / Entwicklung cyber-physischer mechatronischer Systeme (CPMS), zuletzt geprüft am 06.08.2021.

Vesa Linja-aho, 2020. Hybrid and Electric Vehicle Fires in Finland 2015–2019. In: Fires in Vehicles (FIVE) conference. Online Conference. Online verfügbar unter https://www.ri.se/sites/default/files/2020-12/linja-aho-paper-five%20hybrid%20and%20electric%20vehicle%20fires%20in%20finland%202015%e2%80%932019.pdf.